On the effect of impurities on resistivity recovery, short-range ordering, and defect migration in electron-irradiated concentrated Fe - Cr alloys

1997 J. Phys.: Condens. Matter 9 4385

(http://iopscience.iop.org/0953-8984/9/21/006)

J. Phys.: Condens. Matter **9** (1997) 4385–4402. Printed in the UK PII: S0953-8984(97)74083-9

On the effect of impurities on resistivity recovery, short-range ordering, and defect migration in electron-irradiated concentrated Fe–Cr alloys

A L Nikolaev, V L Arbuzov and A E Davletshin

Institute of Metal Physics, UB RAS, 18 S Kovalevskaya Street, GSP-170 Ekaterinburg, 620219, Russia

Received 29 April 1996, in final form 28 October 1996

Abstract. The resistivity recovery of pure and impurity-doped (0.2–1.5% Si, 0.15% C + N) concentrated ferritic Fe–Cr alloys after electron irradiation at 50–60 K has been investigated over the temperature range 110–390 K. A fine recovery spectrum structure consisting of five peaks has been observed over the range 135–230 K. Short-range ordering starts with the onset of vacancy long-range migration. Doping with both types of impurity suppresses the recovery spectrum structure over the range 160–220 K in a similar manner. Additional effects of impurity doping on the resistivity recovery caused by deviation from Matthiessen's rule have been analysed. A stage III peak is found at 210 K, and two peaks—at 175 K and 195 K—are interpreted as being due to the vacancy short-range migration. It is supposed that such a manifestation of short-range vacancy migration is due to a strong immobilization of self-interstitial atoms, and suppression of short-range and long-range defect annealing processes in stage I, according to a configuration-trapping mechanism similar to that of Ag–Zn alloys.

1. Introduction

At present, two sets of experimental data are available on the recovery of residual resistivity (RR) in concentrated BCC Fe–Cr alloys after a low-temperature electron irradiation. The first was obtained by Benkaddour *et al* [1] for high-purity alloys, while the other was obtained by us [2, 3] for alloys with interstitial impurities (0.15 at.% C + N). Although the RR recovery spectra are generally similar, they differ in detail. For example, over the temperature interval 130–210 K, Benkaddour *et al* found only one recovery peak for their alloys (5, 10, 15 at.% Cr)†, and we observed a group of three peaks for the 13.4 at.% Cr alloy [2, 3]. It is difficult to say whether these differences are due to the presence of interstitial impurities, since no systematic data are currently available on the influence of the impurities upon the RR recovery in these alloys.

It was shown elsewhere [3] that silicon atoms suppress the RR recovery in Fe–Cr alloys. In the present study we examined the effect of different silicon concentrations (0.2–1.5 at.%) on RR recovery in a concentrated Fe–16 at.% Cr alloy during annealing after a low-temperature electron irradiation.

In addition to the effect of silicon on the RR recovery, we also estimated the influence of the chromium concentration (11–16 at.%) and interstitial impurities (C + N) in the Fe–13.4 at.% Cr alloy, which was also studied elsewhere [2, 3].

† These data [1] are reproduced in part in figure 5—see later.

0953-8984/97/214385+18$19.50

The data [1–3] were obtained not only for alloys of different purities but also at different irradiation doses (the RR increments were about 2.8 $\mu\Omega$ cm [1] and 0.5 $\mu\Omega$ cm [2] at 70 K). Clearly, the observed differences may result not only from impurities but also from different concentrations of radiation-induced defects. For this reason, we also compared our present data with the data [1] for alloys with similar compositions to ascertain how the initial concentration of defects affects the RR recovery.

2. Defect annealing and RR recovery in concentrated alloys

The annealing of defects and RR recovery in concentrated alloys, and, specifically, in Fe–Cr alloys, have some specific features which can result in a significant modification of the RR recovery for doped Fe–Cr compared to that for pure metals and other alloys.

One feature common to all concentrated alloys arises from the phenomenon of short-range ordering (SRO). Another feature is the possibility of formation of three types of dumb-bell configuration of self-interstitial atoms (IAs)—AA, AB, and BB—in a concentrated AB binary alloy, and their mutual transitions [4, 5].

If a concentrated alloy undergoes irradiation or post-irradiation annealing, migration of non-equilibrium defects enhances the mobility of the atoms, and, as a result, may alter the degree of SRO, and the RR accordingly.

SRO of two types takes place in Fe–Cr alloys [6]. When the chromium concentration is less than 10 at.%, local order is observed. If the chromium concentration exceeds 10 at.%, local clustering (LC) occurs. Concentrations in the vicinity of 10 at.% Cr represent a transition region where the SRO is weakly pronounced. A change in the degree of SRO alters the RR. Specifically, an increase in the degree of LC lowers the RR. It is the LC in Fe–Cr alloys that is responsible for the drop in the RR below the initial level during post-irradiation annealing or under irradiation over a certain temperature interval [1, 2, 7].

A characteristic feature of the contribution of the SRO due to defect migration is its weak dependence (if there is any dependence at all) upon the initial RR increment (the defect concentration or irradiation dose). Since the recovery curves are normalized to the RR increment, the relative contribution of SRO reduces with the increase in the initial concentration of defects [4, 8, 9]. The contribution of the SRO to the RR is usually pronounced during long-range migration of defects [10], so its limitation due to defect–impurity atom interaction can arrest the contribution of the SRO to a large measure even for small impurity concentrations ($\sim$0.1 at.%) [8]. Small impurity concentrations can also reduce the contribution of the SRO by themselves [11].

Ferromagnetic Fe–Cr alloys exhibit yet another feature, which causes renormalization of various contributions to the RR recovery with increasing impurity doping. It is associated with considerable deviations from Matthiessen's rule (DMR), which are observed for ferromagnetic iron alloys [12]. The deviations are explained in terms of the two-current model of Fert and Campbell [12, 13]. The analysis of doping effects on the RR recovery within the two-current model is presented in the appendix.

We shall take into account the above-mentioned features when analysing the experimental results.

3. Experimental procedure

The Fe–16Cr–Si and Fe–11Cr alloys were prepared from carbonyl iron, refined electrolytic chromium, and semiconductor silicon by arc melting in purified argon on a water-cooled

Table 1. Specimen characteristics.

Irradiation run	Alloy (at.% Cr)	Impurity concentration (at.%)	Radiation-induced resistivity (nΩ cm) $\Delta\rho$(70 K)	Radiation-induced resistivity (nΩ cm) $\Delta\rho$(110 K), run I $\Delta\rho$(130 K), run II	Residual resistivity ($\mu\Omega$ cm)
I	Fe–16Cr	< 0.02(C + N)[a]	629	458	13.5 ± 0.3
	Fe–16Cr	0.2Si[b]	683	494	15.9 ± 0.3
	Fe–16Cr	0.5Si[b]	644	465	19.5 ± 0.4
	Fe–16Cr	0.75Si[b]	505	362	25.5 ± 0.5
	Fe–16Cr	1.5Si[b]	271	197	38.2 ± 0.8
	Fe–13.4Cr	0.15(C + N)[a]	607	414	19.5 ± 1.0
II	Fe–13.4Cr[c]	0.15 (C + N)[a]		371	19.5 ± 1.0
	Fe–11Cr	< 0.02(C + N)[a]		560	14 ± 1.0
	Fe–15.7Cr	0.07(C + N)[a]		310	16 ± 1.0

[a]According to nuclear reaction analysis.
[b]According to weighing.
[c]The same sample as in [3].

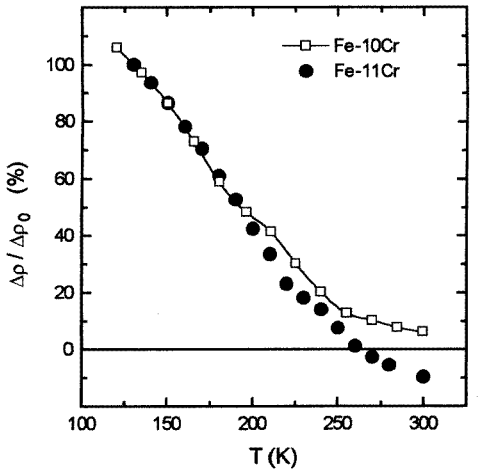

Figure 1. A comparison of the relative resistivity changes during isochronal anneals in Fe–10Cr alloy irradiated at 21 K [1] and in Fe–11Cr alloy irradiated at 110 K. All of the data are normalized at 130 K.

copper hearth. The ingots were forged and cold rolled to the thickness of 50–60 or 200 μm. The Fe–15.7Cr and Fe–13.4Cr alloys were purchased ready made in the form of a cold-rolled foil 200 μm thick. The samples were cut out of the foils using an the electric spark, and were electropolished, and annealed in a 10^{-4} Pa vacuum at 1070 K or 1120 K for 4 h and at 770 K for 0.5 h; this was followed by a rapid cooling. The samples were irradiated with 5.5 MeV electrons to a dose of 10^{18} cm^{-2} in a flow-through helium cryostat [14] in two runs. The irradiation temperature was estimated from the RR recovery spectrum of the iron sample, and (for run I only) by comparing the recovery of Fe–16Cr with the literature data [1] for Fe–15Cr. For run I the estimates give a temperature of about 50–60 K. The alloys in run II were irradiated at 100–110 K; for details refer to [3]. The characteristics of the

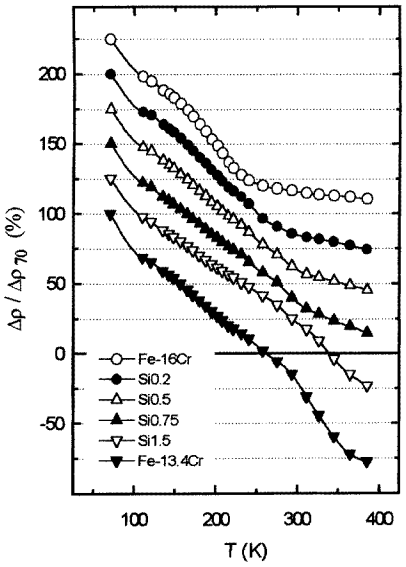

Figure 2. The RR isochronal recovery for Fe–Cr–Si alloys after electron irradiation at 50–60 K; each curve is shifted relative to the next one by 25%.

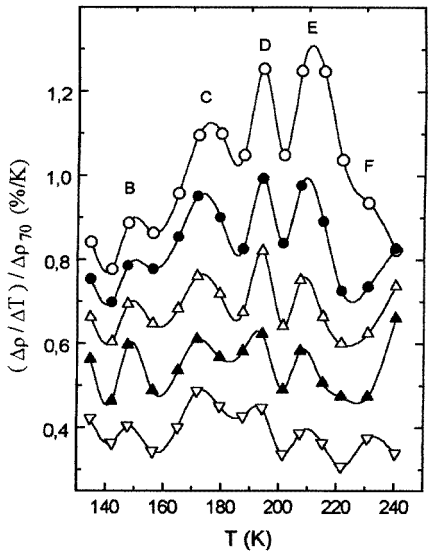

Figure 3. The RR recovery spectra of the Fe–16Cr–Si alloys from figure 2 over the range 135–240 K. The lowest curve relates to the numbers on the *y*-axis, and each following curve is shifted by 0.1% K^{-1}.

samples, and the RR increments after irradiation, and annealing at 70 K and 110 K/130 K are listed in table 1.

Post-irradiation isochronous annealings were realized at an average rate of 1 K min^{-1} in 5–20 K steps. The annealing temperature was controlled by a copper–constantan thermocouple built into the holder. After irradiation the samples in run II were annealed up to 220 K in the irradiation cryostat. Regular fluctuations of the annealing temperature of ± 0.3 K with a period of one minute, because of the automatic control, were observed. The subsequent annealing was performed outside the cryostat (with an accuracy of about 1 K). The last procedure introduced considerable errors in the differentiation of the recovery curves, and that is why the differentiated curves were plotted up to 230 K only. The samples in run I were annealed in the cryostat up to 70 K. During the subsequent annealing, the samples were overheated by accident up to 100–105 K. Then the holder with the samples was transferred without heating above 80 K in a special unit [15] into a helium Dewar, and the samples were further annealed from 110 K in the same unit. The temperature stability was better then 0.1 K (from ± 0.06 K at 100 K to ± 0.025 K at 300–400 K). The RR was measured in a helium flow at 6–7 K in the cryostat, and at 4.2 K, with an accuracy of about 10^{-5} [3].

4. Results

4.1. The effect of Cr concentration and impurity doping on the RR recovery

Figure 1 shows comparative data on the RR recovery for Fe–11Cr and Fe–10Cr [1] alloys over the interval 130 K to 300 K. As can be seen, at 130–190 K the recoveries of the two alloys proceed almost identically. This suggests that the two alloys have defects with

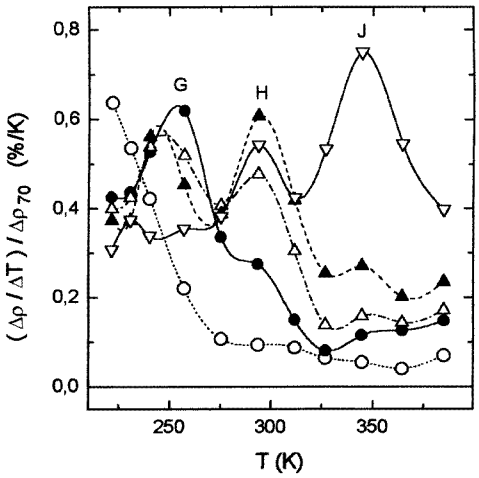

Figure 4. The RR recovery spectra of the Fe–16Cr–Si alloys from figure 2 above 220 K.

similar properties as a result of their having nearly the same concentrations of chromium. An increase in the recovery rate for the Fe–11Cr alloy (as compared to that of Fe–10Cr) above 190 K is indicative of an additional contribution to the RR recovery. This contribution may be due to LC, as the SRO effects are weak in the Fe–10Cr alloy. An examination of figure 1 shows that in the Fe–11Cr alloy this process is rather pronounced, since above 260 K the RR drops below the initial (before irradiation) level.

Figure 2 shows RR recovery curves for run I samples over the interval 70 K to 390 K. As can be seen, the RR increment becomes negative for the pure alloy at temperatures above 240 K, thus indicating the contribution of the LC to the RR recovery. In the case of the silicon-doped samples, this transition shifts to the region of higher temperatures (up to 290 K).

4.2. General remarks on the recovery spectra

Figure 3 depicts differential recovery curves (RR recovery spectra) for Fe–16Cr and Fe–16Cr–Si alloys over the temperature interval 135 K to 260 K. Spectra of the same samples for the interval 220 K to 390 K are shown in figure 4. Figure 5 illustrates the recovery spectrum of Fe–13.4Cr over the interval 135 K to 390 K. In the same figure the comparison of the recovery spectra of the Fe–16Cr alloy and those of Fe–15Cr [1] with different initial concentrations of defects is made. Figure 6 shows recovery spectra of run II samples for the interval between 140 K and 230 K.

Although recovery peaks are represented in figure 6 only by single data points, the reliability of the observed recovery structure is confirmed for Fe–13.4Cr alloy by our data [2] in which the same structure was observed, and by more accurate measurements for the same alloy presented in figure 5, where a similar structure is also observed. However, the peak heights and peak positions observed in [2] and figures 5 and 6 differ markedly. One possible reason for this is the temperature instability†, and the other is a very fine and

† In the above-mentioned case, the temperature fluctuations were periodical. Therefore the inaccuracy of the recovery rate, calculated in a standard manner, may be overestimated (since partial compensation of overheating and underheating effects may take place), and may not explain the observed difference.

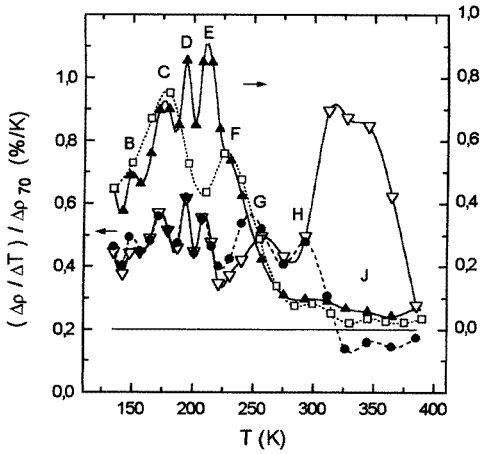

Figure 5. A comparison of the RR recovery spectra for: Fe–15Cr (open squares) [1] and Fe–16Cr (solid upright triangles) after irradiation to different doses (all of the data are normalized at 70 K and $\Delta\rho_{70}$ takes the values 2.8 $\mu\Omega$ cm and 0.63 $\mu\Omega$ cm respectively (upper curves)); and Fe–13.4Cr–0.15(C + N) (inverted open triangles) and Fe–16Cr–0.5Si (solid circles) (lower curves).

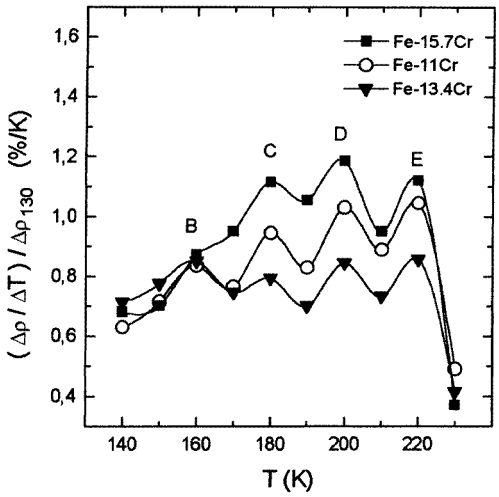

Figure 6. The RR recovery spectra of Fe–Cr alloys after electron irradiation at 100–110 K.

tight recovery structure clearly resolved in figures 3 and 5 with a 5–7 K annealing step. Therefore small shifts in annealing temperature points (3–5 K) in different experiments, and a sufficiently large annealing step (10 K) can result in a marked change of the measured recovery rate. That is why we compare recovery rate data for different alloys in figure 6 only within run II at the same temperatures, where the relative inaccuracies in peak heights are the same for all samples. Peak D in figure 3 is also represented by a single data point, but its height (for Fe–16Cr) exceeds that for neighbouring points by 20%, with the maximum error in the peak height being about 3%. The reliability of this peak is also confirmed by its good reproducibility in our further experiments [16].

4.3. The effect of Cr concentration and impurity doping on RR recovery spectra

An examination of figures 3, 5, and 6 shows that over the temperature interval 135 K to 230 K all of the alloys studied (runs I and II) have the same structure of the recovery spectra, comprising four peaks. We labelled the peaks B, C, D, and E. (The label A is assigned to the peak observed at 85–90 K [1, 2].) The recovery spectrum of the undoped pure alloy (figure 3) exhibits a poorly resolved peak at 230 K (F), and the same peak is observed for the Fe–15Cr alloy [1] (figure 5), which is interpreted [1] as the peak of stage III (the onset of the vacancy long-range migration).

As is seen from figures 3 and 6, the heights of the peaks B, C, D, and E depend on both the concentration of chromium and that of the impurity in the alloy. Peak B is least sensitive to these factors. Its amplitude rises—but only slightly—when the chromium concentration is increased from 11% to 15.7% (figure 6), remains unchanged if up to 0.75% Si is added, and reduces markedly only after doping with 1.5% Si (figure 3). The peaks C, D, and E grow considerably (figure 6) in going from Fe–11Cr to Fe–15.7Cr. A general increase in the RR recovery over the given temperature interval was also observed [1] when the chromium concentration was raised. The Fe–13.4Cr alloy does not obey this regularity, a fact which is due to the rather high content of interstitial impurities in this alloy. Like silicon, these impurities weakly influence peak B, and reduce the heights of the peaks C, D, and E (figures 5 and 6).

A characteristic feature of all of the peaks from B to F is the suppression of their height with increasing impurity doping.

A comparison of the recovery rate of Fe–16Cr and that of Fe–15Cr [1] having a higher initial concentration of radiation defects (figure 5) shows that a much greater recovery rate is observed for our alloy over the interval 190 K to 230 K. An increase in the RR recovery with decreasing initial concentration of defects is a marker of the LC.

4.4. RR recovery above stage III

At temperatures above 230 K (figure 4) a group of three peaks is observed for silicon-doped alloys: G (230 K–255 K), H (300 K), and J (340 K). Peaks H and J are observed also for the Fe–15Cr alloy [1] and can be traced in our Fe–16Cr alloy. Peak G is not resolved for these alloys, but the possibility of its existence cannot be excluded, since a broad shoulder of peak F is observed in this temperature interval. In contrast to lower-temperature peaks, these peaks are not suppressed with increasing Si concentration, and can even grow.

For the Fe–13.4Cr alloy doped with interstitial impurities (figure 5) the location of the peaks is somewhat different: peaks are observed near 320 K and 340 K. In addition, these peaks have a much greater amplitude.

5. Discussion

5.1. General remarks

Our alloys differ markedly from the high-purity alloys [1] as regards their purity, as is seen from the RR values (13.5 $\mu\Omega$ cm for our Fe–16Cr alloy, 11.9 $\mu\Omega$ cm and 12.3 $\mu\Omega$ cm for Fe–10Cr and Fe–15Cr [1] respectively; see [17]). Considering the purity of the materials and the control melts of iron obtained under the same conditions, it can be concluded that the concentration of residual impurities in our alloys does not exceed several hundredths of one per cent. As is seen from figure 5, the RR recovery rate is on average lower for the Fe–16Cr alloy than for the purer Fe–15Cr alloy [1], except in the 190–230 K interval, and

in the regions where the LC occurs. This effect is probably due to the presence of residual impurities. However, it is several times weaker than the changes caused by introduction of 0.2 at.% Si. Hence the presence of residual impurities should hardly affect the results obtained.

From the experimental data it follows that for our alloys the interstitial impurities are not the cause of the difference (mentioned in the introduction) between the recovery spectra in [1] and [2], as these impurities lead only to suppression of the observed spectrum structure. A comparison of our data and the data from [1] revealed a possible reason for the difference within the range 190–230 K: a dose-dependent contribution of the LC at these temperatures. Another possible reason is a fine and tight structure of the recovery spectrum with a typical 15–20 K peak width. The authors of [1] used a 15 K step, and it is therefore no surprise that some fine features of the structure of the RR recovery spectrum were not resolved.

5.2. Stage III recovery

As was mentioned above, peak F was interpreted [1] as the peak of stage III, and later the authors of [17] considered positron lifetime data as a confirmation of their conclusion. But according to those data the two-component lifetime is observed even after annealing at 200 K. This means that stage III processes start near this temperature, and our peaks D and E should also be suspected of belonging to stage III. It is well known that in concentrated alloys the onset of long-range defect migration is accompanied by the appearance of SRO effects [8, 9, 18], which are especially well pronounced for vacancy migration. As can be seen in figure 5, this is not the case for peak F. The choice should be made between peaks D and E. As can be clearly seen in figure 1, the LC effects are very weak near the peak D temperature, and are well pronounced near peak E. Since the behaviour of vacancies is similar for all Fe–(5–15) at.% Cr alloys [17] can be concluded that it is most probably peak E that corresponds to the stage III peak. From this viewpoint, peak D is not connected with vacancy long-range migration, and its probable nature is discussed below.

Stage III RR recovery should involve two processes: defect reactions (annihilation, clustering, and vacancy–impurity-atom complex formation) and LC. As is known, silicon [19] and interstitial impurities (C + N) [20] in iron retard the annealing of vacancies through the formation of vacancy–impurity-atom complexes. Taking into account the similarity of the properties of vacancies in pure iron and in Fe–Cr alloys, and the similar structure of the alloys and iron, it can be expected that these impurity atoms will behave in a similar manner in the alloys. Since in our alloys the impurity concentration is always much higher than the defect concentration ($\sim 5 \times 10^{-5}$), almost all of the vacancies should be captured by impurity atoms during long-range migration; therefore RR recovery due to other defect reactions, the LC, and its contribution to RR recovery (due to the strong limitation of the vacancy migration paths) should be suppressed. The suppression should be almost complete as long as such complexes are stable and immobile. This may be expected to be valid for our alloys at stage III peak temperatures, since in Fe such complexes are stable and immobile at least up to 260 K. In metals, the formation of vacancy–impurity-atom complexes may be accompanied by a drop in the vacancy contribution to the RR (up to tens per cent of the vacancy contribution to the RR). Therefore in a normal alloy with a high impurity concentration, vacancy trapping should lead to a saturation of stage III suppression over a certain range of impurity concentration.

But if the impurity concentration is about one atomic per cent, the probability that vacancies are produced within the capturing volume of the impurity atoms becomes sufficiently large, and these vacancies can form vacancy–impurity-atom complexes after

a few jumps within a capturing volume (short-range trapping) at temperatures below that of the onset of long-range migration†. That is why a progressive reduction in the stage III peak height may be observed with increasing doping in normal alloys, since the vacancy fraction which can be trapped during long-range migration is reduced. The two-current model predicts an additional reduction for Fe-based alloys as a result of the renormalization of contributions to the RR from vacancy–impurity-atom complexes and Frenkel pairs (FP) with increasing impurity concentration (see the appendix). So, two factors—the total capturing volume of all of the impurity atoms, and renormalization—determine the suppression of the recovery peak (induced by the dominant formation of vacancy–impurity-atom complexes) with increasing doping in the alloys.

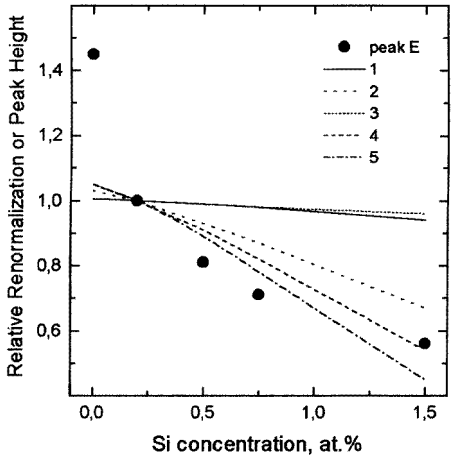

Figure 7. Observed relative values of the peak E reduction (solid circles) and the renormalization of the RR recovery calculated within the two-current model (lines) as functions of the silicon concentration, and for different values of the model parameters (for details see point (5) of the appendix): 1: $z_{i-V} = 0.46, z_c = 0.3$; 2: $z_{i-V} = 0.46, z_c = 0.0$; 3: $z_{i-V} = 0.35, z_c = 0.2$; 4: $z_{i-V} = 0.35, z_c = -0.1$; 5: $z_{i-V} = 0.46, z_c = -0.2$; $z_{i-V} = 0.35, z_c = -0.15$.

Figure 7 presents a comparison between the observed relative reduction in the peak E height and the renormalization calculated according to the model (for details, see the appendix). One should keep in mind that neighbouring peaks may overlap significantly owing to a tight recovery spectrum structure, and that the observed height of peak E may also depend upon the heights of neighbouring peaks. The greatest effect may result from peak D, but its height lowers similarly to that of peak E with increasing doping. Therefore overlapping will not substantially affect the relative reduction in peak E. From such a comparison one can determine the interval of reasonable values for the model parameters.

It can be expected that the short-range vacancy trapping will still be negligible in Fe–16Cr–0.2Si alloy, and, as can be seen from figure 7, for reasonable values of the parameters the model predicts a small renormalization effect for this alloy compared with the pure alloy. Therefore a significant difference from the experimental data obtained for the alloys (figure 7) should be attributed to the suppression of contributions from the LC and other defect reactions, owing to the dominant reaction of vacancy trapping. So the behaviour of peak E with doping corresponds to that expected for the stage III peak.

† There is some analogy with close-pair recombination.

5.3. Recovery above stage III

If one compares the heights of the stage III peaks (due to complex formation) in Fe–16Cr–0.2Si and Fe–0.04Si [21], their ratio is about 3. If the peak overlap effects are taken into account, this ratio may reduce nearly to half of that value. If the fraction of retained vacancies at the onset of the complex formation is the same in the alloy and iron, the above ratio (according to model calculations with reasonable parameters; see point (5) of the appendix) should be about one tenth or lower. Even if the approximate character of our model calculations is taken into account, such a discrepancy is too large, and may only be understood if the fraction of retained vacancies in the alloy and iron differs significantly (it is several times larger) at the onset of the complex formation. Since total RR recovery in Fe–16Cr and Fe–16Cr–0.2Si differs only slightly at this temperature, the same conclusion may be valid for the pure alloy too.

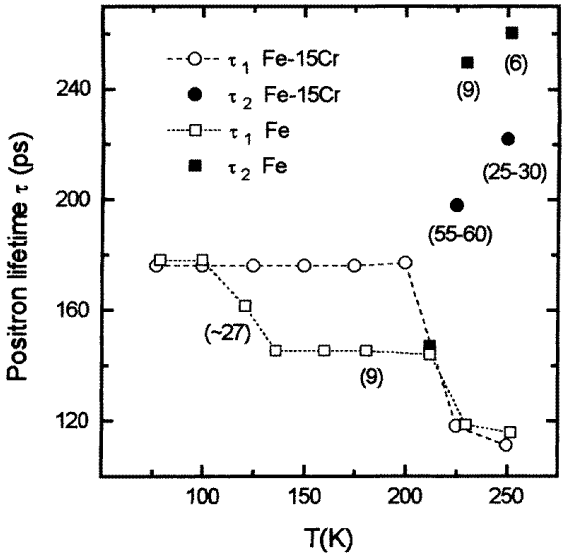

Figure 8. A comparison of the positron lifetime recovery after 3 MeV low-temperature electron irradiation in Fe ($\Phi = 3 \times 10^{18}$ cm^{-2}) [20] and in Fe–15Cr alloy ($\Phi = 2.5 \times 10^{18}$ cm^{-2}) [17]. Estimates of the vacancy concentration (free or clustered) in ppm are given in brackets for some temperatures. For Fe, these data were taken from [20], except those for 120 K, and the others were calculated according to [20] and taking the positron trapping rates of vacancy clusters to be equal for the alloy and iron.

To verify this conclusion, in figure 8 we compare the literature data [17, 20] on the positron lifetime recovery in iron and Fe–15Cr alloy irradiated with almost the same dose under the same conditions. For the lifetime near 100 K, part of stage I—corresponding to the defect recombination—is clearly seen for iron. In the alloy, no changes in the lifetime are observed up to 220 K, a fact which may be indicative of a suppression of the recombination processes. The numbers of clustered vacancies in the alloy and iron were calculated at temperatures above 220 K. The calculated values are given in the figure. As can be seen, the number of vacancies in the alloy is five times larger than that in iron. From this fact it may be concluded that the fraction of retained vacancies at the onset of stage III in the alloy is significantly larger than that in iron.

Since at temperatures below that of stage III the LC contribution to the RR recovery is

absent, and considering the similarity of the lattice structures, one can use the fraction of retained RR increment to bring into an approximate correlation the processes for the alloy and those for pure iron. For pure Fe–15Cr alloy [1], at the onset of stage III the fraction of retained RR increment is about 22%, a value which corresponds to the RR increment fraction at the onset of IA long-range migration in pure iron [22], provided that no loss in the alloy defect resistivity below stage III takes place. Since a loss in specific FP resistivity is probable when IAs are captured by Cr atoms [23], the retained fraction of the alloy RR increment may correspond to a lower-temperature sub-stage in iron.

All of these facts are in qualitative agreement with the results of our model calculations. Thus one may conclude that the recombination of defects at temperatures below that of stage III is strongly suppressed in the Fe–Cr alloys compared to that in pure iron. This means that stage I in the alloys is not completed, and that the same fraction of IAs (as vacancies) should be retained at the onset of stage III. Such a situation may be due only to a strong limitation of the IA mobility below the stage III temperatures.

A gradual suppression of close-pair (sub-stage I_{D1}), correlated (sub-stage I_{D2}), and long-range (sub-stage I_E) migration processes in stage I is observed in Fe doped with more than 1% Cr [23, 1]. These processes can still be detected in alloys with Cr concentrations up to 10% [1], but are almost fully suppressed in Fe–13.4 at.% Cr [2] and Fe–15 at.% Cr [1]. An attempt was made to interpret the RR recovery in Fe–Cr alloys (0–3 at.% Cr) [23] in terms of a mobile mixed dumb-bell formation, migration, and configuration trapping of IAs, like in Ag–Zn alloys [4].

The main difference between these two cases is that Zn in Ag is an undersized impurity, but Cr in Fe is an oversized one [1, 23]. It is generally assumed that the formation of a mobile mixed dumb-bell is very unlikely in the case of oversized impurity, owing to an increase in the dumb-bell configuration energy. For this reason, defect annealing in Fe–(5–15) at.% Cr alloys [1], contrary to what is proposed in [23], is discussed in terms of IA configuration energy increase when changing from FeFe to FeCr and CrCr dumb-bell configurations. Correlated and long-range migration of IAs is reduced, due to the restricted possibilities for FeFe dumb-bell migration, and is shifted towards higher temperatures ($\sim$160 K for Fe–5Cr and $\sim$180 K for Fe–(10–15)Cr), at which a transition from an FeFe to an FeCr configuration becomes possible.

It should be noted at once that these data on the LC effects starting only with vacancy long-range migration contradict [1], since long-range IA migration with Fe–Fe to Fe–Cr dumb-bell transformations will lead to LC effects at 180 K. Also according to [1], the peak at 160 K (peak B in our representation) for the Fe–5Cr alloy shifts to the neighbourhood of 180 K (peak C) as the chromium concentration is raised to 10%. In actual fact, as is evident from figures 3, 5, and 6, peak B is found in the recovery spectra of the alloys containing 11% to 16% chromium, and a quite different peak appears at 180 K. The different natures of these peaks becomes evident: their response to silicon doping is completely different (figure 3); and peak B exhibits a weak dependence on the chromium concentration, while peak C increases rapidly (figure 6). For this reason, given a large annealing step, the resolution of peak B is impaired progressively with increasing chromium concentration, as can be seen for the example of the Fe–15.7Cr alloy shown in figure 6, and peak B is not resolved in [1].

Then a suppression of the RR recovery, which is observed [1] in the temperature range of stage I for iron (100–120 K) when the chromium concentration is raised from 5 at.% to 15 at.%, is followed by the appearance and growth of peak C rather than the displacement and growth of peak B. So the processes which are suppressed at 100–120 K start only at 180 K (peak C). From what has been said above, it follows that peaks C and D are due, most probably, to close-pair and correlated defect migration. In our further speculations,

for the sake of simplicity, we shall not distinguish close-pair and correlated processes, and we consider them both as short-range migration processes.

Short-range trapping of vacancies at impurity atoms should take place for our impurity concentrations, and give rise to additional recovery peak(s) below stage III temperatures, a situation which is not observed in the experiment. Such peak(s) will not appear additionally (or will not be resolved as additional) if the recovery spectrum already has peak(s) corresponding to vacancy short-range migration. In neutron-irradiated iron, RR recovery peaks due to short-range vacancy migration within cascades were observed at 150 K and 180 K [24]. Taking into account the similarity of the vacancy properties in iron and in the alloy, sub-stage C may be attributed to vacancy short-range migration.

Thus the stage I short-range recombination, which is suppressed in iron, shows up in Fe–Cr alloys near 180 K owing to vacancy short-range migration. Correlated migration is known to be very sensitive to the initial distribution of radiation-induced defects. Generation of small defect cascades consisting of two or three neighbouring FP cannot be excluded for our electron irradiation energy (5.5 MeV). Correlated vacancy migration within such cascades may give rise to an additional recovery peak which should be absent in alloys irradiated with lower-energy electrons. This may be the reason for the appearance of peak D in our experiments. The comparison of our data with those of [1] shows that only a few per cent of defects may be generated within cascades. So, in Fe–Cr alloys, two short-range vacancy migration stages are possible after our irradiation: short-range migration within FP (peak C), and short-range migration between neighbouring FP within a cascade (peak D).

In the case of doped alloys, short-range recombination will be gradually replaced by vacancy–impurity-atom complex formation, and the degree of the replacement will depend on the ratio of the number of lattice sites within the total capturing volume of the impurity atoms (which is proportional to the impurity concentration) and the total number of jumps for all of the vacancies. Then the RR recovery consists of two parts: due to recombination, and due to vacancy–impurity-atom complex formation. The total RR recovery should decrease with increasing doping, the decrease being slower than in stage III. This is actually observed in the experiment (figure 3).

A unique situation can be observed for Fe–13.4Cr–0.15(C + N) and Fe–16Cr–0.5Si alloys in figure 5. Peaks C, D, and E coincide almost completely. Such a situation may be expected if the total capturing volumes of impurity atoms and vacancy fractions involved in C, D, and E sub-stage processes are close for these alloys. Close vacancy fractions may be anticipated for the two alloys, since the difference in RR recovery is less than 4% at 160 K (figure 2). The fact that the total capturing volumes of the impurity atoms are nearly the same means that the trapping radius is larger for interstitial impurity atoms than for silicon ones. This is reasonable, since interstitial impurity atoms are known to produce more lattice distortions than substitutional ones. Under these conditions the fractions of vacancies trapped at impurity atoms in stage III are similar in the two alloys. The coincidence of stage III peak heights means that—coincidentally—the RR recoveries due to vacancy–impurity-atom complex formation are close in the two alloys. But the accidental coincidence of stage III peak heights for the two alloys requires a coincidence of C and D peak heights as regards their vacancy nature, since the fractions of vacancies trapped in sub-stages C, and D and the corresponding RR recovery should be close in the alloys too.

A similar coincidence of C and D peaks is very unlikely in the case of their IA nature, since in iron the interactions of IAs with interstitial impurities and silicon atoms are different [22, 21]. Therefore the observed coincidence is a very strong argument in favour of a vacancy nature of C, D, and E sub-stages.

The behaviour of peak B with doping differs from that of the peaks induced by vacancy

migration. That is why the appearance of the peak may be ascribed to IA migration. Since silicon atoms are known to form mixed dumb-bells with IAs in iron [21], it may be anticipated that IAs interact with silicon atoms in Fe–Cr alloys too. But the observed RR recovery over 70–165 K, and the height of peak B are weakly sensitive to doping up to 0.75% Si (figures 2 and 3). Only at 1.5% Si concentration does the height of peak B drop abruptly. If such a drop were due to the interaction of IAs with Si atoms near the peak temperature, a gradual suppression of the peak height would be observed with increasing doping. Therefore it may be thought that such a drop is due to low-temperature processes, and further discussion needs additional information on low-temperature recovery which is not yet available. One should keep in mind that the observed effect of silicon on the height of peak B does not indicate directly an interaction between IAs and silicon atoms, since doping can exert an indirect influence through renormalization.

The above-presented analysis of the RR recovery in the alloys agrees with the interpretation given in [23], according to which IA configuration trapping takes place in the Fe–Cr system. But vacancy short-range migration has never been observed in FCC alloys with such a type of trapping [4, 9, 10]. We think that this is a specific feature of iron-based alloys. As compared to FCC metals, in the iron the homological temperature of the IA migration and vacancy migration is strongly shifted towards high temperatures and low temperatures respectively. So, in Fe–Cr alloys the homological temperature interval between the beginnings of IA migration and short-range vacancy migration is too narrow, and the processes of short-range IA migration, which in FCC alloys with configuration trapping usually extend between the stage I and stage III temperatures [4], are unable to develop.

Our findings contradict the conclusion reached in [25], according to which the IA migration energy in the Fe–10Cr alloy equals 0.35 eV (i.e. differs little from the value for Fe). This conclusion is drawn from the data on the nucleation and growth of interstitial loops obtained using a high-voltage electron microscope at 300–570 K. The IA migration energy is determined assuming that the concentration of freely migrating IAs depends on their recombination with vacancies under quasistationary conditions. However, when metals and alloys undergo irradiation, the quasistationary state is realized only for a limited period of time [26], which depends on the mobility of the fast species of the Frenkel pair (IAs [25]), and may be estimated as the time required for IAs to migrate to the average distance between point defect sinks. Under the conditions of [25], the distance cannot exceed the size of the irradiation zone, i.e. about 1 μm. Given the IA migration energy of 0.35 eV, even at the lowest irradiation temperature (300 K [25]) the duration of the quasistationary state is less than a second. Thus this state cannot be observed, and, hence, the assumptions are invalid. Taking into account later reports on close values of vacancy mobilities in iron and Fe–Cr alloys [17, 28], the difference in the loop accumulation kinetics, which was found for the Fe–10Cr alloy at 300–570 K and iron at 300 K [25], may attest to considerably different properties of IAs in the alloy and iron.

5.4. Recovery above stage III

The subsequent evolution of defects in the alloys at temperatures above that of stage III depends on the nature of the secondary defects formed as a result of the processes at lower temperatures. But only limited information concerning defect states is currently available. It is known that in the pure alloy, vacancy clusters are formed [17]. From the above analysis it can be concluded that in doped alloys, vacancies are bound into complexes. It can be anticipated that lightly doped alloys contain mainly vacancy–single-silicon-atom

complexes, and in heavily doped alloys complexes including several neighbouring silicon atoms (multiple trapping) can be formed. It can be also concluded that IAs are strongly immobilized, probably due to the configuration-trapping mechanism [4]. Nothing can be said on the interaction of IAs with silicon and interstitial impurity atoms.

In contrast to the low-temperature case, here the LC contribution may be dominant in the RR recovery, and be the main determining factor as regards the intensity of the recovery processes above stage III. The intensity behaviour is not simple, and cannot be discussed now since opposite tendencies result from increasing doping: on the one hand, the fraction of the LC contribution should increase due to renormalization (see the appendix); but on the other hand, it may be suppressed as a result of multiple trapping, and may be reduced directly by doping [11].

Therefore, further annealing processes should start when dissociation of defects from bound states takes place. Since a correlation between FP partners should increase during vacancy capture with increasing doping, it may be expected that the recovery peak caused by dissociation will be shifted towards low temperatures with increasing doping [21]. Such behaviour is likely to be observed for peak G (figure 4). It shifts from 255 K (Fe–16Cr–0.2Si) to 230 K (Fe–16Cr–1.5Si). The dissociation of simple vacancy–silicon atom complexes is observed at 260 K in iron [19], and therefore it is highly probable that a similar process takes place in our alloys at 230–255 K.

We do not discuss the behaviour of peak F, since data are currently lacking. It is difficult to give even a probable interpretation of peaks H and J, since it is not clear whether the coincidence of the H and J positions for pure and doped alloys (where vacancy-type defects are of different nature) is coincidental or a genuine feature. Nothing can be said on whether the peak at 320 K in Fe–13.4Cr–0.15(C + N) alloy represents the shifted peak H or not. If it does, it is not known what the nature of the shift is: due to the difference in the chromium concentration or due to the difference in the dopant type. Without additional experimental information, discussion of these problems is valueless.

5.5. Concluding remarks

Although in the present interpretation we have managed to bring into agreement data on defect properties in Fe–Cr alloys obtained in different experiments and by different techniques, some reasonable caution as regards such agreement should be exercised, and possible ways of looking for additional evidence should be discussed.

We treat the positron lifetime data [17] as annihilation parameters, being the same for both iron and the alloy. It is not inconceivable that this is not appropriate, resulting in the differences discussed. Measurements analogous to [17] but made under a lower irradiation dose and with an unsaturated positron lifetime would permit the observing of actual variations in the vacancy concentration during annealing after a low-temperature irradiation, and allow the obtaining of additional information about IA properties.

We have compared the RR recoveries after different irradiation doses for alloys with different purities, and with slightly varying chromium concentrations subjected to different irradiations at different temperatures. That is why dose dependence measurements on the same alloys are necessary, and such work is in progress [16]. It will not only permit us to ascertain the dose effects in sub-stage E, but also allow us to verify our interpretation of the processes below the stage III temperature.

6. Conclusions

The experiments yielded the following important results.

(1) A fine RR recovery structure comprising five peaks over the temperature range 135–230 K is observed for Fe–Cr alloys.

(2) Stage III is observed at 210 K, and it is accompanied by the onset of a short-range-ordering process.

(3) Two peaks—at 175 K and 195 K—are caused by short-range vacancy migration.

(4) Vacancies form complexes with silicon and interstitial impurity atoms.

(5) It follows from the observed features of the vacancy migration that the interstitial atoms are strongly immobilized, probably due to the configuration-trapping mechanism.

Acknowledgments

The work was carried out with the financial support of the International Science Foundation (grants RG2000 and RG2300). One of the authors (ALN) thanks Dr C Dimitrov and Dr C Corbel for providing numerical data on resistivity and positron annihilation recovery, and is grateful to Professor Yu P Irkhin and Professor V Yu Irkhin for stimulating discussions.

Appendix. The effect of impurity doping on the Frenkel pair (FP), vacancy–impurity-atom complex, and local clustering contributions to the residual resistivity (RR), and RR recovery within the two-current model

(1) According to the two-current model [12, 13], in the alloys there are two groups of conduction electrons—those with spin up (↑) and those with spin down (↓) (relative the internal magnetic field)—that may be scattered by the lattice defects in different ways. Each lattice defect of the ith species is characterized by two contributions to the RR: $\rho_{i\uparrow}$ and $\rho_{i\downarrow}$. Matthiessen rule is valid separately for each group, and the resistivities of different groups in the absence of spin mixing are summed according to the law of parallel connection of conductors:

$$\rho^{-1} = \left(\sum_i \rho_{i\downarrow}\right)^{-1} + \left(\sum_i \rho_{i\uparrow}\right)^{-1}.$$

According to appendix I in [27], an alternative set of parameters, instead of $\rho_{i\downarrow}$, $\rho_{i\uparrow}$, may be used for calculation of the alloy RR within the two-current model:

$$z_i = (\rho_{i\downarrow} - \rho_{i\uparrow})/(\rho_{i\downarrow} + \rho_{i\uparrow}) \qquad R_i = \rho_{i\downarrow} + \rho_{i\uparrow}.$$

Hereafter, ρ_i denotes the resistivity (not specific) of the ith species. Then, neglecting the spin-flip scattering, the total RR is given by

$$\rho = (1 - z^2)R/4 \tag{A1}$$

with $z = \sum_i z_i R_i / \sum_i R_i$ and $R = \sum_i R_i$.

(2) The contribution of defects to the RR for small concentrations of defects in iron-based alloys can be written as [27]

$$\rho_D/(\rho_D)_{Fe} = 1 + (z_s - z_D)^2/(1 - z_D^2) = (1 + z_s^2 - 2z_s z_D)/(1 - z_D^2) \tag{A2}$$

where $(\rho_D)_{Fe}^{-1} = (\rho_{D\downarrow})^{-1} + (\rho_{D\uparrow})^{-1}$, which, within certain limits, may be considered as a defect resistivity in pure iron, and z_s and z_D are the parameters for the non-irradiated alloy and the defect respectively.

The value of z for impurities in iron is†: $z_F(\mathrm{FP}) = 0.82$ [23]; $z(\mathrm{Cr}) = -0.46$; $z(\mathrm{Si}) = 0.7$ [13]. The exact z-value for interstitial impurities is not known, but considering the similarity of the scattering potentials it should be close to that of the IA (or FP)‡. As can be easily seen, doping of the Fe–Cr alloy (z_s is negative) with Si or interstitial impurities (z is positive) will cause an increase in z_s, and, as a result, a reduction of $(z_s - z_F)^2$ and the FP resistivity (see table A1). Unfortunately, the data of the present paper cannot be directly compared with the estimates, because of the inhomogeneous irradiation.

Table A1. Numerical estimates for Fe–Cr–Si alloys.

Alloy	z_s	RR(calc)/ RR(meas)	FP resistivity	LC resistivity
Fe–Cr	−0.46		100%	100%
+0.2 at.% Si	−0.32	100%	83%	100.3%
+0.5 at.% Si	−0.17	104%	66%	100.7%
+0.75 at.% Si	−0.07	92%	57%	102%
+1.5 at.% Si	0.12	82%	41%	111%

(3) Such concentrated alloys as ours should be treated in the two-current model as multicomponent alloys containing Cr atoms that are single, coupled, and tripled (and so on) at the neighbouring lattice sites as scattering centres, with their own z- and R-parameters, which are unknown. To determine the z- and R-parameters of Fe–16Cr alloy we have used the following idea. Since the FP specific resistivity is approximately the same for the Fe–Cr alloys with 5 to 15 at.% (∼170 $\mu\Omega$ cm/at.%) [28], one can conclude that the z_s-parameter is approximately the same for these alloys, and can use the usual value of z(Cr). The R-parameter is calculated from the RR value of the purest alloy [17] according to (A1). For other calculations concerning Fe–Cr–Si alloys (see table A1), parameters for Si [13] have been used. The agreement between the calculated and measured RR values is satisfactory, but it is likely that our model calculations slightly underestimate Si doping effects, and probably some corrections to the parameters for Si are necessary.

(4) LC may affect the resistivity by changing both R and z. The LC results in an increase in the number of neighbouring Cr atoms, and since such a process leaves the z-parameter almost unchanged, it should affect the resistivity through the variation of R. If the direct effect of impurities on the LC is neglected, relative changes in the resistivity caused by variation of R (during the LC) for the impurity-doped ($\delta\rho_i$) and basic Fe–Cr ($\delta\rho_0$) alloys can be easily calculated, as follows:

$$\delta\rho_i/\delta\rho_0 = (\mathrm{d}\rho_i/\mathrm{d}R_0)/(\mathrm{d}\rho_0/\mathrm{d}R_0) = 1 + [R_{imp}/(R_{imp} + R_0)]^2(z_{si} - z_{s0})^2/(1 - z_{s0}^2) \qquad \text{(A3)}$$

where $\mathrm{d}R_0$ is the variation of R due to the LC, which is the same in basic and doped alloys; R_0 is the R-parameter for the basic alloy, and R_{imp} is the contribution of impurities to the R-parameter; z_{si} and z_{s0} are z-parameters for doped and basic alloys respectively. Estimates show (see table A1) that the LC contribution corrections are negligible even for a heavily doped alloy.

(5) Let us define as z_{i-V} the parameter for the impurity-atom–vacancy pairs which are going to form complexes (according to (A1)) and as z_c the complex parameter. Then,

† On page 769 in [13] are listed the values of the most commonly used α- and ρ-parameters, where $\alpha = \rho_\downarrow/\rho_\uparrow$, and $\rho^{-1} = (\rho_\downarrow)^{-1} + (\rho_\uparrow)^{-1}$; $z = (\alpha - 1)/(\alpha + 1)$.

‡ Our estimate of the specific resistivity for interstitial impurities in Fe–Cr alloys (about 50 $\mu\Omega$ cm/at.%) supports this suggestion.

according to (A2), the change in the RR due to the complex formation can be expressed as

$$\Delta\rho_c = [(1 + z_s^2 - 2z_s z_{i-V^2})/(1 - z_{i-V^2})](\rho_{i-V})_{Fe} - [(1 + z_s^2 - 2z_s z_c)/(1 - z_c^2)](\rho_c)_{Fe}. \tag{A4}$$

The relative change in the RR due to the complex formation can be written as

$$(\Delta\rho_c/\rho_F)/(\rho_{i-V}/\rho_F)_{Fe} = [(1 + z_s^2 - 2z_s z_{i-V})/(1 - z_{i-V}^2) - r(1 + z_s^2 - 2z_s z_c)/(1 - z_c^2)](1 - z_F^2)/(1 + z_s^2 - 2z_s z_F) \tag{A5}$$

with $r = (\rho_c/\rho_{i-V})_{Fe}$.

If $r = 1$, the quantity $\Delta\rho_c/\rho_F$ is proportional to

$$(z_{i-V}^2 - z_c^2)\frac{(1 + z_s^2 - 2z_s z^*)}{(1 + z_s^2 - 2z_s z_F)} \qquad \text{with} \qquad z^* = \frac{(1 + z_{i-V} z_c z_s)}{(z_{i-V} + z_c)}. \tag{A6}$$

If $z_{i-V} z_c z_s \ll 1$ and $0 < z_{i-V} + z_c < 1$ and $z_{i-V} - z_c > 0$, then $z^* > z_F$, and a drop in RR and the RR recovery peak due to complex formation may be observed, and the peak height will be systematically renormalized (reduced) with increasing z_s (and impurity concentration) due to DMR effects. For our impurities, r is approximately the same, and is less than unity [22, 21], and this will lead to a weakening of the effect. The decrease in z and R during the complex formation corresponds to a RR drop in normal metals. The expression (A5) gives the ratio between the RR drop for the doped Fe–Cr alloy and that for doped iron if the fraction of vacancies (of the total produced by irradiation) taking part in complex formation is the same. From (A5) it is possible to estimate the effect of doping on the peak height renormalization for the alloy, and the relative fractions of retained vacancies in the alloy and iron. For the numerical estimation we approximate vacancy parameters with values for Ti and V ($z_V = -0.2; -0.8$ [13]) as two extreme cases [23] (for Si and a vacancy, $z_{i-V} = 0.46$–0.35; $R_{i-V} = 55$–57 $\mu\Omega$ cm and $(\rho_{i-V}/\rho_F)_{Fe} = 0.45$–$0.48$). The r-parameter was taken as 0.85, which corresponds approximately to a loss of 40% of the vacancy contribution due to complex formation. The corresponding numerical estimates are presented in the text.

References

[1] Benkaddour A, Dimitrov C and Dimitrov O 1987 *Mater. Sci. Forum* **15–18** 1263

[2] Arbuzov V L, Davletshin A E, Klotsman S M, Nikolaev A L, Altovskii I V, Grigoryan A A and Votinov S N 1989 *Vopr. At. Nauki Tekh., Ser. Fiz. Radiats. Povrezhden. Radiats. Materialoved.* **1** 3

[3] Nikolaev A L and Arbuzov V L 1994 *Fiz. Met. Metalloved.* **78** 437

[4] Maury F, Lucasson P, Lucasson A, Vajda P, Balanzat A, Beretz D, Halbwachs M and Hillairet J 1984 *Radiat. Eff.* **82** 141

[5] Boquet J L 1986 *Acta Metall.* **34** 571

[6] Mirebeau I, Hennion M and Parette G 1984 *Phys. Rev. Lett.* **53** 687

[7] Arbuzov V L, Davletshin A E, Druzhkov A P, Nikolaev A L, Klotsman S M, Altovskii I V and Grigoryan A A 1990 *Vopr. At. Nauki Tekh., Ser. Fiz. Radiats. Povrezhden. Radiats. Materialoved.* **3** 18

[8] Dimitrov C and Dimitrov O 1984 *J. Phys. F: Met. Phys.* **14** 793

[9] Vaessen P, Lengeler B and Shilling W 1984 *Radiat. Eff.* **81** 277

[10] Bartels A, Kemkes C and Lucke K 1985 *Acta Metall.* **33** 1887

[11] Dimitrov O and Dimitrov C 1986 *J. Phys. F: Met. Phys.* **16** 969

[12] Fert A and Campbell I A 1976 *J. Phys. F: Met. Phys.* **6** 849

[13] Campbell I A and Fert A 1982 *Ferromagnetic Materials* ed E P Wohlfarth (Amsterdam: North-Holland) p 760

[14] Arbuzov V L and Davletshin A E 1992 *Cryogenics* (*ICEC Suppl.*) **32** 183

[15] Davletshin A E and Nikolaev A L 1996 *Prib. Tekh. Eksp.* (5) 149 (Engl. Transl. 1996 *Instrum. Exp. Tech.* **39** (5))

[16] Nikolaev A L *et al* 1997 *J. Phys.: Condens. Matter* to be submitted
[17] Dimitrov C, Benkaddour A, Corbel C and Moser P 1991 *Ann. Chim. (France)* **16** 319
[18] Bartels A, Bartusel D and Lucke K 1987 *Phys. Status Solidi* a **104** 315
[19] Moser P, Corbel C, Lucasson P and Hautojarvi P 1987 *Mater. Sci. Forum* **15–18** 925
[20] Vehanen A, Hautojarvi P, Johanson J and Yli-Kauppilla J 1982 *Phys. Rev.* B **25** 762
[21] Maury F, Lucasson A, Lucasson P, Moser P and Loreaux Y 1985 *J. Phys. F: Met. Phys.* **15** 1465
[22] Takaki S, Fuss J, Kugler H, Dedek U and Schultz H 1983 *Radiat. Eff.* **79** 87
[23] Maury F, Lucasson P, Lucasson A, Faudot F and Bigot J 1987 *J. Phys. F: Met. Phys.* **17** 1143
[24] Matsui H, Takehana S and Guinan M W 1988 *J. Nucl. Mater.* **155–157** 1284
[25] Yoshida N, Yamaguchi A, Muroga T, Miyamoto Y and Kitajima K 1988 *J. Nucl. Mater.* **155–157** 1232
[26] Sizman R 1968 *J. Nucl. Mater.* **69–70** 386
[27] Maury F, Lucasson A, Lucasson P, Moser P and Faudot F 1990 *J. Phys.: Condens. Matter* **2** 9291
[28] Dimitrov C, private communication